

Predicting Perception of the Wagon Wheel Illusion

Patrick Martineau, Martin Aguilar, and Leon Glass*

Department of Physiology, McGill University, Montreal, Quebec, Canada

(Received 8 October 2008; published 9 July 2009)

Stroboscopic illumination of a rapidly rotating disk with radial spokes leads to a range of different stationary and moving images as the angular rotation frequency of the disk and the strobe frequency are varied. We compare predictions from the standard correlation model of motion perception with a model based on phase locking observed during periodic stimulation of an integrate-and-fire nonlinear oscillator. The close agreement between theoretical predictions and experimental observations suggests the possibility that periodic forcing of nonlinear neural oscillations may play a role in motion perception.

DOI: 10.1103/PhysRevLett.103.028701

PACS numbers: 42.66.Si, 05.45.-a, 87.18.Tt, 87.80.Ek

One of the curiosities of motion pictures is the apparent illusory slow forward or backward rotation of wheels—initially observed in moving covered wagons in old westerns and now still familiar in car chases. This wagon wheel illusion, whose history can be traced back to Faraday [1,2], results from the aliasing arising from the repetition frame rate of the motion picture and the rotation frequency of the wheel. Modern studies of the wagon wheel illusion elicited by stroboscopic illumination of rotating disks with radial spokes [3–6] demonstrate a number of different percepts as the strobe frequency, rotation frequency, and number of radial spokes are varied. However, they do not offer an adequate theoretical basis for predicting the percept under different presentation conditions.

To illustrate the wagon wheel illusion, we consider a clockwise rotating disk with 4 spokes that is illuminated by a strobe [6,7] (Fig. 1). We set the strobe frequency such that the disk rotates by 84° between each flash. Figure 1 shows the three images generated by the first three flashes on the left and the superimposition of the first three images on the right. Provided the strobe frequency is sufficiently high, one would observe a counterclockwise rotation with a velocity of 6° per strobe flash rather than the much more rapid clockwise rotation. In general, as the strobe frequency varies, we observe the wagon wheel illusion at several different resonant stimulation frequencies as illustrated in Fig. 2 and subsequent figures. The apparent correspondence between Fig. 2 and organization of phase locking dynamics observed during experimental [8,9] and theoretical [10–16] studies of periodic forcing of nonlinear cardiac and neural oscillators has led us to reconsider the wagon wheel illusion. In this Letter, we present experimental studies of the wagon wheel illusion and compare the observations with predictions of percepts using two different theoretical models: a “standard” correlation analysis model and a new model based on periodically forced nonlinear oscillators. This analysis suggests novel mechanisms for neural processing of stimuli leading to the wagon wheel illusion.

Consider a white disk with N narrow, dark, radial spokes rotating clockwise at a frequency ω that is illuminated by a strobe that delivers brief flashes of light with a period τ_s . The recurrence time τ_r is the time required for one radial spoke to make $1/N$ of a revolution in a clockwise direction. Thus, $\tau_r = 1/\omega N$. Edgerton observed that a stationary pattern should appear provided $\tau_s = n\tau_r$, where n is an integer [7]. However, additional resonance conditions may also occur if

$$m\tau_s = n\tau_r, \quad (1)$$

where m and n are both integers [3,6]. When this resonance holds, the observed number of spokes is expected to be mN . Equation (1) applies over limited rotation speeds and flash frequencies for low values of m and n [3–6]. However, since given any value of τ_s/τ_r it will always be possible to find values m and n such that

$$0 < \left| \frac{\tau_s}{\tau_r} - \frac{n}{m} \right| < \epsilon \quad (2)$$

for arbitrarily small ϵ , one might expect to see stationary patterns for arbitrary ratios of τ_s/τ_r . But this would preclude observation of the wagon wheel illusion and does not correspond to what is observed.

The limited experimental studies of the wagon wheel illusion to date [3–6] do not provide adequate experimental data to test theoretical predictions as the strobe frequency,

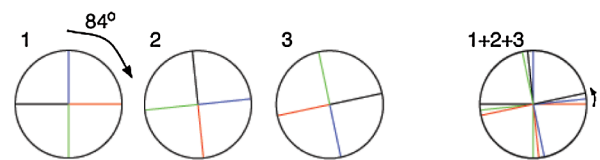


FIG. 1 (color online). Illustration of the wagon wheel illusion. The first three panels illustrate three successive positions of a disk with 4 spokes during a clockwise rotation of 84° per strobe flash. The right panel shows the superimposition of the three images, leading to the wagon wheel illusion with a counterclockwise rotation of 6° per strobe flash.

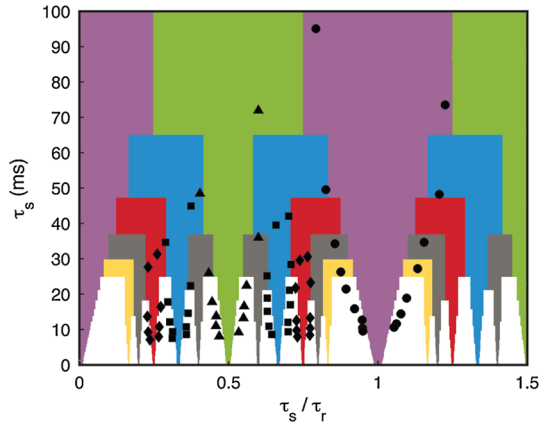


FIG. 2 (color online). Predicted zones for the wagon wheel illusion based on the correlation function analysis with superimposed experimental data collected from one of the authors in a determination of the boundaries of the resonance zones. τ_s is the time between strobe flashes, and τ_r is the recurrence time. The experimentally determined borders for a rotating disk with 4 spokes are indicated by the superimposed symbols: $m = 1$ (circles); $m = 2$ (triangles); $m = 3$ (squares); $m = 4$ (diamonds); $m = 6$ (star). For a disk with N spokes, the colored zones have mN spokes: $m = 1$ (purple); $m = 2$ (green); $m = 3$ (blue); $m = 4$ (red); $m = 5$ (gray); $m = 6$ (yellow). We assume $T = 200$ ms.

rotation speed, and number of spokes are varied. To provide such data, we have carried out experiments using stimuli consisting of rotating disks subtending 7.5° of visual field with 4, 8, or 16 radial spokes viewed in a dark room at a distance of 141 cm. Each spoke subtended an angle of 9.8 min of visual field at the outer diameter of the disk. The disks were mounted on a computer controlled stepper motor (AM23-144-2, Advanced Micro Systems, Nashua, NH) capable of rotational speeds of 600 rpm. We used a digital strobe (Shimpo DT-311A, Electromatic Equipment Co., Cedarhurst, NY) which operates in a range of 40–35 000 flashes per minute. Flash duration and power were 10–40 μ s and 10 W, respectively.

Figure 2 shows the results of experiments to determine the boundaries of the resonances carried out on one of the authors using a disk with 4 spokes. For several different rotation speeds, we first adjusted τ_s to give a stationary pattern based on Eq. (1) for several low values of m and n . Then, for a fixed rotation speed, the strobe frequency was changed eliciting the wagon wheel illusion until the subject was no longer able to visually track one spoke for one full rotation. To determine the velocity, we measure the time required for one spoke to complete 10 rotations. As we describe below, this provides a check on the experimental observations and theory.

In discussing theoretical models for motion perception, we employ the Farey series. The Farey series of order M , \mathcal{F}_M , is the ascending sequence of rationals i/j where $j \leq M$ [17]. For example, $\mathcal{F}_6 = 0, 1/6, 1/5, 1/4, 1/3, 2/5, 1/2, \dots$

The standard theoretical model for motion perception assumes that the visual system computes a correlation of the visual scene with itself at different times [18–20]. The percept then corresponds to a moving image that is most consistent with the correlation function, where slower moving images are more strongly favored. In order for the perceived number of spokes to be a multiple of the number of rotating spokes, there must be a correlation of two or more images, each of which represents not just the image from a single strobe flash but images from multiple strobe flashes. Following earlier studies, we assume that there is a visual persistence time T , where $T \approx 130$ – 220 ms, and all images that occur within a time interval T can be summed [4,21]. Consequently, the maximum number of flashes that can be summed is

$$M = \lfloor T/\tau_s \rfloor, \quad (3)$$

where $\lfloor x \rfloor$ is the largest integer smaller than x .

We compute the correlation functions of the visual image during the stroboscopic illumination of a clockwise rotating disk with N spokes to predict the percept. For a given τ_s and τ_r we first determine M from Eq. (3). Then we determine the value of \mathcal{R} , $\mathcal{R} \in \mathcal{F}_M$, that minimizes the quantity $|\frac{\tau_s}{\tau_r} - \mathcal{R}|$. The correlation analysis predicts that we will observe a rotating pattern of mN spokes, where m is the denominator of \mathcal{R} . The illusory wagon wheel rotation frequency ω_w is

$$\omega_w = \frac{\frac{\tau_s}{\tau_r} - \mathcal{R}}{N\tau_s}, \quad (4)$$

where a negative sign signifies counterclockwise rotation and a positive sign signifies clockwise rotation. The agreement of the experimentally measured velocity with this theoretical prediction serves as a check on the experimentally determined boundaries in Figs. 2 and 3.

In Fig. 2, the colored regions show the predicted zones up to \mathcal{F}_6 based on the computation of the correlation function and assuming that $T = 200$ ms. The computed zones are in good qualitative agreement with computed zones based on the correlation analysis. However, the boundaries of the resonance zones in Fig. 2 show a striking organization similar to Arnold tongues observed during the periodic forcing of nonlinear oscillators. An Arnold tongue refers to a tongue-shaped region in frequency-amplitude space of the periodic forcing function in which there is phase locking typified by a constant rational ratio between the number of cycles m of the periodic stimulus and the number of cycles n of the perturbed oscillator. For fixed stimulus amplitude, as the stimulation period increases, the ratio n/m is typically a nondecreasing function [10–15].

Theoretical models for periodically forced biological oscillators often assume an “integrate-and-fire” mechanism (Fig. 3) [11–15]. In the absence of stimulation, the activity periodically increases to a threshold 1, fires an impulse, and then decreases. We model the stimulus induced by the strobe as a vertical bar from the baseline of

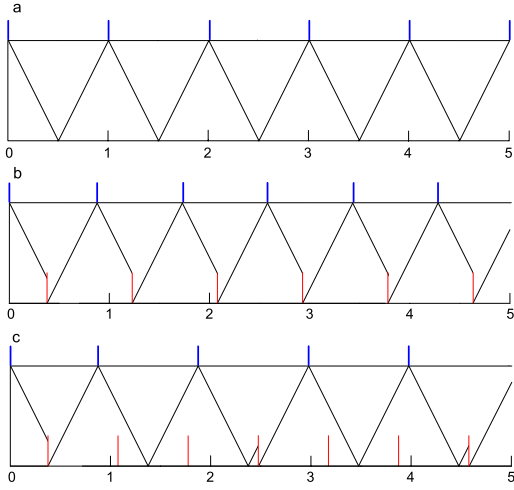


FIG. 3 (color online). Model of a neural oscillator that is periodically stimulated [13]. The stimulus induced by the strobe is modeled by red vertical bars from the baseline of length d and with a (dimensionless) time interval between the stimuli of τ_s/τ_r . The firing of the neuron occurs when the activity reaches threshold, indicated by a blue vertical bar. (a) No stimulation; (b) 1:1 entrainment with $d = 0.3$ and $\tau_s/\tau_r = 0.8$; (c) 3:2 entrainment with $d = 0.3$ and $\tau_s/\tau_r = 0.7$.

length d and with a time interval between the stimuli of τ_s/τ_r . If the stimulus occurs when the activity $\leq d$, the activity will reset to the baseline and then continue upward. Figure 3 shows two different behaviors that arise by changing τ_s/τ_r while keeping $d = 0.3$. For $\tau_s/\tau_r = 0.8$ there is a 1:1 synchronization between the stimulus and the oscillator, whereas for $\tau_s/\tau_r = 0.7$ there is 3:2 synchronization in which there are 3 stimuli for every 2 firing events.

We are able to compute the boundaries of the entrainment zones [13]. We set the oscillator to have period 1 and define zero phase to occur when the model neuron fires. Defining φ_i , $0 \leq \varphi_i \leq 1$, as the phase of the i th stimulus in the cycle of the oscillator,

$$\varphi_{i+1} = \begin{cases} \frac{1}{2} + \frac{\tau_s}{\tau_r} (\text{mod } 1) & \text{if } \frac{1-d}{2} < \varphi_i < \frac{1+d}{2}, \\ \varphi_i + \frac{\tau_s}{\tau_r} (\text{mod } 1) & \text{otherwise.} \end{cases}$$

From this we compute that, for

$$\left| \frac{\tau_s}{\tau_r} - \frac{n}{m} \right| \leq \frac{d}{2m}, \quad (5)$$

there is a stable cycle of period m in which $\varphi_m = \varphi_0$, $\varphi_j \neq \varphi_0$ for $1 \leq j < m$. For a given value of d , calling M the maximum value of m , we find

$$M = \lfloor 2/d \rfloor. \quad (6)$$

In an $m:n$ resonance zone, the rotation frequency is

$$\omega_w = \frac{\varphi^* - 0.5}{mN\tau_s}, \quad (7)$$

where φ^* is the phase of the cycle for which $\frac{1-d}{2} < \varphi^* < \frac{1+d}{2}$. Consequently, in this model the phases of the periodic

stimuli in the neural oscillation are related to the velocity of the wagon wheel rotation.

In order to compare this model with experimental data on a scale comparable to Fig. 2, we equate (3) and (6), to find $d = 2\tau_s/T$. For $T = 200$ ms ($d = \tau_s/100$) there is close agreement between the computed locking zones and superimposed data (Fig. 4).

By adjusting the value of the integration time T , we can obtain better agreement of the two models with experiment. We computed the optimal value of T by minimizing the mean square distance σ^2 of the experimentally determined points with $\tau_s < 60$ ms from the theoretically computed boundaries. Although the optimal value of T for the correlation model is $T \approx 180$ ms ($\sigma^2 \approx 0.022$) and $T \approx 230$ ms ($\sigma^2 \approx 0.015$), the differences are not great, and, for ease of comparison, we have presented both models assuming the same integration time and have plotted the boundaries assuming an intermediate value $T = 200$ ms. The steplike appearance of the boundaries in the correlation model arises from the floor function in Eq. (3) which assumes a fixed integration time for all conditions.

We further compare theory with experiments based on an early study reporting the perceived direction of the wagon wheel illusion, the apparent velocity, and the number of spokes for clockwise rotating disks with 4, 8, or 16 spokes with rotation speed constant at 2 Hz, and variable strobe frequency in 15 subjects [4]. Since there was often uncertainty in the number of spokes (Table 2 in Ref. [4]), we have rechecked these data using two trained observers. In Fig. 5, we present the data based on our own observations, which in several cases differ from the original reports. In the supplementary material, we reproduce the original tables from Ref. [4] along with our data and ω_w computed from Eq. (4) [22]. For points lying near theoretically computed boundaries of zones, there are often competing percepts in which both clockwise and counter-clockwise percepts are possible. There is close agreement

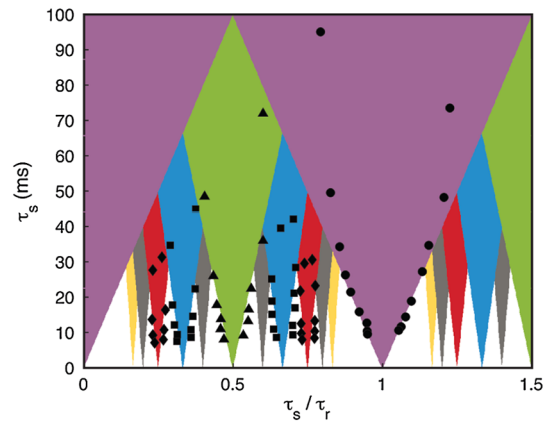


FIG. 4 (color online). Theoretically computed locking zones from the neural oscillator model in Fig. 3 with superimposed experimental data collected from one of the authors in a determination of the boundaries of the resonance zones. We assume $T = 200$ ms. Symbols are as in Fig. 2.

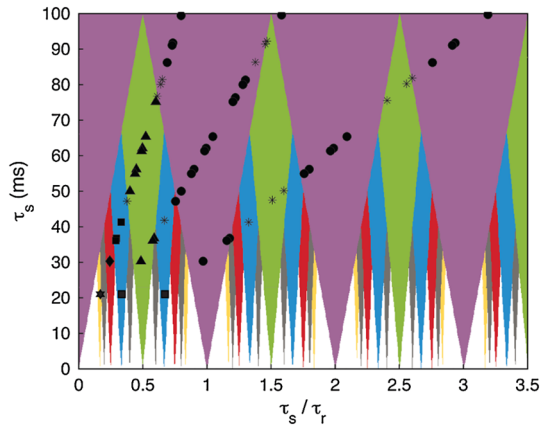


FIG. 5 (color online). Theoretically computed locking zones from the neural oscillator model in Fig. 3 and superimposed data points for clockwise rotating disks with 4, 8, or 16 spokes with rotation speed constant at 2 Hz and variable strobe frequency (see text and supplementary material [22]). The asterisks represent points of multistability. We assume $T = 200$ ms. Symbols are as in Fig. 2.

of the data with the predictions based on the periodically forced nonlinear oscillator.

Our results suggest several directions for further experimental and theoretical studies. As the boundary of a resonance zone was approached, the image would often become unstable, a clear perception of the wagon wheel illusion was often difficult, and multistability was often observed. The mechanisms underlying the shift between these different percepts are not known. Hysteresis, eye movement, and attention all appear to play a role. Thus, further psychophysical studies are needed, especially to resolve the qualitative differences in theoretical predictions of the correlation model (Fig. 2) and the periodically forced oscillator model (Figs. 4 and 5) in the neighborhood of boundaries of the resonance zones. If the neural processing underlying perception of the wagon wheel illusion is due to entrainment of neural oscillators in the brain, then experimental recordings of neural activity should show time-dependent changes in the phases of neural activity relative to the timing of stroboscopic pulses as the strobe frequency is varied. Since experimental studies have analyzed time-dependent changes of neural activity during perception tasks in monkeys [23,24], it would be interesting to extend these studies using stimuli eliciting the wagon wheel illusion.

Although the suggestion that periodically forced nonlinear oscillators may be playing a role in the perception of the wagon wheel illusion appears natural to those with a knowledge of nonlinear dynamics, previous studies of the wagon wheel illusion have not identified such a mechanism [3–6]. The quantitative agreement of the periodically forced oscillator model with experimental data suggests that the periodic stimulation of a neural oscillator may

indeed play a role in the computations underlying human motion perception.

We thank S. Biuno, M. Beauchamp, W. Kucharski, and P. Glass for technical assistance and C. Pack and E. Cook for helpful conversations. This research has been funded by NSERC. A demonstration of the wagon wheel illusion by K. Brecher (Boston University) and S. Gorlin (MIT) as part of the Boston University NSF funded “Project LITE: Light Inquiry Through Experiments” is at Ref. [25].

*glass@cnd.mcgill.ca

- [1] M. Faraday, *J. R. Inst. Great Britain* **1**, 205 (1831) [reprinted in *Experimental Researches in Chemistry and Physics* (Taylor & Francis, London, 1859), p. 291].
- [2] N. J. Wade and D. Heller, *Psych. Res.* **60**, 227 (1997).
- [3] R. M. Shymko and L. Glass, *Opt. Eng.* **14**, 506 (1975).
- [4] D. Finlay, P. Dodwell, and T. Caelli, *Perception* **13**, 237 (1984).
- [5] D. J. Finlay and P. C. Dodwell, *Percept. Psychophys.* **41**, 29 (1987).
- [6] D. Purves, J. A. Paydarfar, and T. J. Andrews, *Proc. Natl. Acad. Sci. U.S.A.* **93**, 3693 (1996).
- [7] H. E. Edgerton, *Electronic Flash Strobe* (McGraw-Hill, New York, 1970).
- [8] L. Glass, M. R. Guevara, J. Bélair, and A. Shrier, *Phys. Rev. A* **29**, 1348 (1984).
- [9] K. Aihara and G. Matsumoto, in *Chaos*, edited by A. V. Holden (Manchester University Press, Manchester, 1986), p. 257.
- [10] V. I. Arnold, *Geometrical Methods in the Theory of Ordinary Differential Equations* (Springer, New York, 1988).
- [11] J. P. Keener, F. C. Hoppensteadt, and J. Rinzel, *SIAM J. Appl. Math.* **41**, 503 (1981).
- [12] L. Glass and R. Perez, *Phys. Rev. Lett.* **48**, 1772 (1982).
- [13] J. Bélair, *J. Math. Biol.* **24**, 217 (1986).
- [14] L. Glass, *Nature (London)* **410**, 277 (2001).
- [15] P. H. E. Tiesinga, *Phys. Rev. E* **65**, 041913 (2002).
- [16] H. Croisier, M. R. Guevara, and P. C. Dauby, *Phys. Rev. E* **79**, 016209 (2009).
- [17] G. H. Hardy and E. M. Wright, *An Introduction to the Theory of Numbers* (Clarendon Press, Oxford, 1960).
- [18] W. Reichardt, in *Sensory Communication*, edited by W. A. Rosenblith (MIT Press, Cambridge, MA, 1961), p. 303.
- [19] E. H. Adelson and J. R. Bergen, *J. Opt. Soc. Am. A* **2**, 284 (1985).
- [20] Y. Weiss, E. P. Simoncelli, and E. H. Adelson, *Nat. Neurosci.* **5**, 598 (2002).
- [21] R. Efron and D. N. Lee, *Am. J. Psychol.* **84**, 365 (1971).
- [22] See EPAPS Document No. E-PRLTAO-103-064930 for the original tables from Ref. [4] along with our data and ω_w computed from Eq. (4). For more information on EPAPS, see <http://www.aip.org/pubservs/epaps.html>.
- [23] W. Bair and J. A. Movshon, *J. Neurosci.* **24**, 7305 (2004).
- [24] P. E. Williams and R. M. Shapley, *J. Neurosci.* **27**, 5706 (2007).
- [25] <http://lite.bu.edu/vision/applets/Motion/Wagon/Wagon.html>.